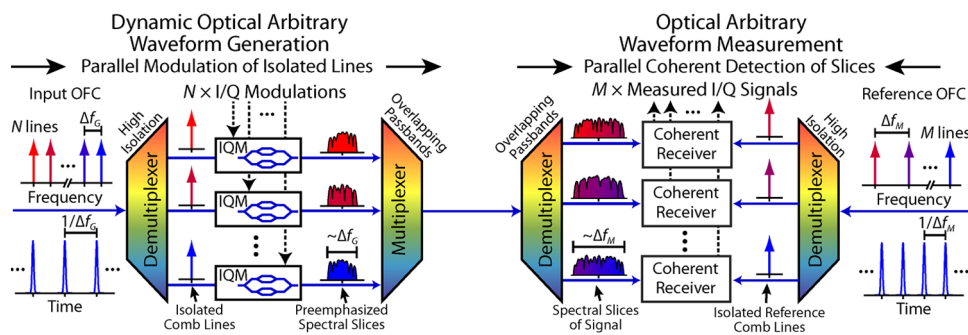


Demonstration of a Flexible Bandwidth Optical Transmitter/Receiver System Scalable to Terahertz Bandwidths

Volume 3, Number 6, December 2011

David J. Geisler, Student Member, IEEE
 Nicolas K. Fontaine, Member, IEEE
 Ryan P. Scott, Member, IEEE
 S. J. B. Yoo, Fellow, IEEE



DOI: 10.1109/JPHOT.2011.2171931
 1943-0655/\$26.00 ©2011 IEEE

Demonstration of a Flexible Bandwidth Optical Transmitter/Receiver System Scalable to Terahertz Bandwidths

David J. Geisler, *Student Member, IEEE*, Nicolas K. Fontaine, *Member, IEEE*, Ryan P. Scott, *Member, IEEE*, and S. J. B. Yoo, *Fellow, IEEE*

Department of Electrical and Computer Engineering, University of California, Davis, CA 95616 USA

DOI: 10.1109/JPHOT.2011.2171931
1943-0655/\$26.00 © 2011 IEEE

Manuscript received September 1, 2011; revised October 3, 2011; accepted October 5, 2011. Date of publication October 17, 2011; date of current version November 4, 2011. This work was supported in part by the Defense Advanced Research Projects Agency and the Space and Naval Warfare Systems Center under Optical Arbitrary Waveform Generation (OAWG) Contract HR0011-05-C-0155, under National Science Foundation Electrical, Communications and Cyber Systems (ECCS) Grant 1028729, and under the CISCO Systems, Inc. University Research Program. Corresponding author: S. J. B. Yoo (e-mail: yoo@ece.ucdavis.edu).

Abstract: This paper demonstrates a flexible bandwidth-modulation-capable and bandwidth-scalable transmitter and receiver technique based on dynamic optical arbitrary waveform generation (OAWG) and measurement (OAWM). This technique generates and receives broadband arbitrary optical waveforms by dividing the waveform spectrum into overlapping spectral slices of bandwidth manageable with existing electronics. The OAWG transmitter produced 2-ns, 60-GHz data waveforms using only 5.5 GHz of analog bandwidth by coherently combining six 10-GHz spectral slices. Measurements were performed using an OAWM receiver with two 30-GHz spectral slices using 15 GHz of analog bandwidth. Experimental demonstrations verify the modulation format independence and flexible bandwidth capabilities of OAWG transmitters and OAWM receivers through the generation of the following waveforms: binary phase-shifted keying (BPSK), coherent wavelength division multiplexing (CoWDM) with 5 and 15 BPSK subcarriers, and orthogonal frequency division multiplexing (OFDM) with 54 BPSK subcarriers. All waveforms had a bit-error-rate performance better than 7.8×10^{-5} .

Index Terms: Coherent communication, pulse shaping, ultrafast measurements.

1. Introduction

To meet the exponentially increasing demand for Internet bandwidth, solutions for next-generation optical transmission systems must efficiently utilize available bandwidths with scalability beyond Terahertz bandwidths. Recently, flexible bandwidth networking has emerged as a possible method to effectively use the available bandwidth [1]. A potential solution based on flexible bandwidth networking can increase network utilization by using variable bandwidth channels ranging in bandwidth from subwavelength to superwavelength channels to match link demand with allocated bandwidth. Additionally, the modulation format can be adaptively changed to ensure successful transmission under varying link conditions [1]–[3]. This approach has been shown to reduce or completely eliminate the spectral guard bands or the stranded bandwidth that occurs in cases of partially utilized channels. However, a major challenge for realizing transmitters and receivers for high-capacity flexible bandwidth networking is overcoming the electronic bottleneck to enable scaling of single channel bandwidths using existing electronics.

Multicarrier solutions such as coherent wavelength division multiplexing (CoWDM) [4] and orthogonal frequency division multiplexing (OFDM) [5]–[8] have been proposed as possible implementations of flexible bandwidth networking. These solutions rely on the generation of many low speed subcarriers to form broadband data waveforms using lower speed modulators. CoWDM maintains orthogonality between closely packed subcarriers by individually modulating each tone from a set of coherent subcarrier tones, and setting the subcarrier symbol rate equal to the subcarrier spacing. OFDM systems utilize an inverse Fourier transform at the transmitter and a Fourier transform at the receiver to ensure orthogonality between subcarriers. A guard band is often necessary to compensate for chromatic dispersion at the cost of a slight spectral efficiency penalty, but techniques such as no-guard-band OFDM can eliminate the need for guard bands [9]. Both CoWDM and OFDM systems can change the modulation format of individual subcarriers but lack the ability for arbitrary control over subcarrier symbol rate and spacing with a single physical architecture.

A more general method for broadband waveform generation is based on dynamic optical arbitrary waveform generation (OAWG). The generated arbitrary optical waveforms can include data waveforms in both single carrier modulation formats and multicarrier modulation formats such as CoWDM and OFDM. Here, “dynamic” refers to continuous waveform generation, as opposed to line-by-line pulse shaping, which has time duration limitations typically on the order of tens of picoseconds [10]–[14]. In particular, spectral-slice based dynamic OAWG can create continuous, high-fidelity waveforms that overcome the limitations of rapidly updating the modulations to a line-by-line pulse shaper [15], [16]. Spectral-slice dynamic OAWG utilizes the parallel synthesis and coherent combination of many lower bandwidth spectral slices to create broadband data waveforms [17], [18]. In contrast to multicarrier systems, the spectral slice bandwidth is not related to the subcarrier bandwidth of generated waveforms. This removes any restrictions on the subcarrier bandwidth and its modulation format and is only limited by the total operational bandwidth of the OAWG transmitter. The parallel nature of this transmitter structure enables bandwidth scalability without increasing the bandwidth demand on the supporting electronics. The complementary receiver is optical arbitrary waveform measurement (OAWM), in which a broadband, continuous bandwidth waveform is divided into many spectral slices for parallel measurement using independent digital coherent receivers [19].

Previously, we demonstrated 2×10 GHz and 3×10 GHz spectral slice signal generation to create single carrier data waveforms [20], which were detected using a typical digital coherent receiver. Here, we bring together a dynamic OAWG transmitter and OAWM receiver into a single system with an optical bandwidth of 60 GHz that demonstrates the bandwidth scalability of this technique to 1 THz and beyond. The transmitter generated 6×10 GHz spectral slices to form the complete 60 GHz signal, and the receiver measured waveforms using 2×30 GHz spectral slices [21]. We build on our initial demonstration by also showing the capability to satisfy the needs of flexible bandwidth transmitters and receivers through the generation and measurement of single-carrier waveforms in addition to multicarrier CoWDM and OFDM waveforms. In contrast to other transmitter and receiver structures, dynamic OAWG transmitters and OAWM receivers do not need to match spectral slice bandwidth to subcarrier baud rate to ensure orthogonality between subcarriers.

This manuscript is organized as follows: Section 2 presents the concept of spectral-slice dynamic OAWG transmitters and OAWM receivers. In detail, we describe the mechanism by which the spectral slice technique enables the generation and detection of both single and multicarrier data waveforms. Section 2 also details the necessary digital signal processing (DSP) operations for generating and detecting data waveforms encoded in any modulation format. Section 3 presents experimental results that verify high-fidelity generation and detection of 60 GHz, 2-ns single carrier, five-subcarrier CoWDM, 15-subcarrier CoWDM, and 54-subcarrier OFDM data waveforms. Section 4 concludes the paper.

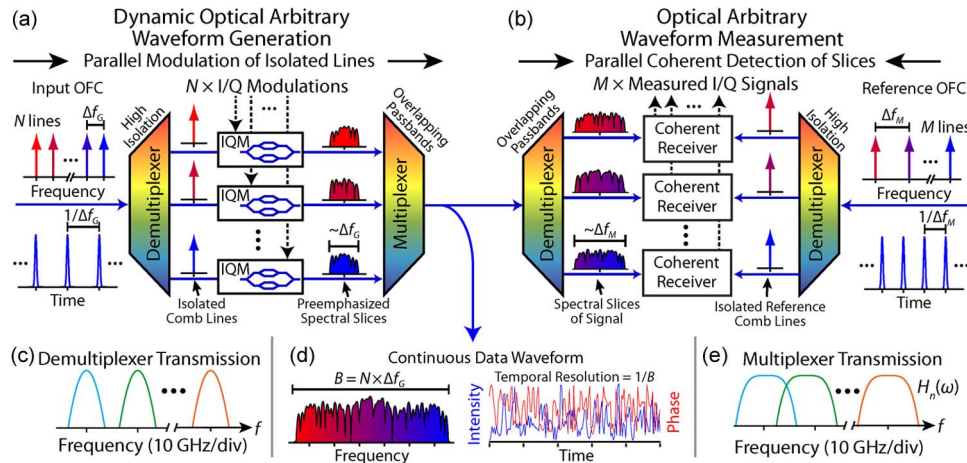


Fig. 1. Spectral slice (a) OAWG and (b) OAWM techniques for bandwidth scalable generation and detection of arbitrary modulation format data transmissions. (c) Demultiplexer and (e) multiplexer transmission functions. (d) Example continuous bandwidth, and complex data waveform.

2. Flexible Bandwidth Transmission System Based on Dynamic OAWG and OAWM

A flexible bandwidth transmission system based on a dynamic OAWG transmitter and an OAWM receiver can coherently generate and receive data waveforms by dividing the total waveform bandwidth into spectral slices of manageable bandwidth. This enables the use of currently available technology in a bandwidth-scalable manner to operate over large amounts (> 1 THz) of continuous bandwidth. In this fashion, a dynamic OAWG transmitter creates large bandwidth waveforms through the parallel generation and coherent combination of many lower speed spectral slices (e.g., ~ 10 GHz optical bandwidth) [20]. Similarly, an OAWM receiver coherently divides the data waveform into spectral slices (e.g., ~ 40 GHz optical bandwidth) that are individually detected with parallel digital coherent receivers [19]. For example, a 100-GHz transmission system could be implemented using 10×10 GHz spectral slices at the transmitter and 4×25 GHz spectral slices at the receiver.

Fig. 1(a) shows how dynamic OAWG can generate N spectral slices, each with bandwidth Δf_G , to form an aggregate output waveform with a total bandwidth of $N \times \Delta f_G$. Dynamic OAWG begins with a coherent optical frequency comb (OFC), which is spectrally demultiplexed with narrow passbands [see Fig. 1(c)] placing each comb line at a separate spatial location. A set of in-phase and quadrature-phase modulators (I/Q modulators) each with a bandwidth of Δf_G apply temporal I/Q modulations to broaden the comb lines to create the spectral slices. Coherently combining the spectral slices using a gapless spectral multiplexer [see Fig. 1(e)] with broad overlapping passbands ensures a continuous bandwidth output waveform [see Fig. 1(d)]. Also, incorporating compensation for the multiplexer transmission as a preemphasis of the modulation signals ensures high-fidelity waveform generation after the multiplexer [20].

Analogously, Fig. 1(b) illustrates how an OAWM receiver characterizes waveforms through the coherent detection of M spectral slices, each with bandwidth Δf_M . For the receiver, a reference OFC with M -lines spaced at Δf_M provides a reference tone for the detection of each spectral slice [19]. The reference comb lines are isolated using a spectral demultiplexer with narrow and discrete passbands [see Fig. 1(c)], and the signal is divided into spectral slices using a separate gapless spectral demultiplexer [see Fig. 1(e)] that has strongly overlapping passbands. Each reference comb line is then used to detect the corresponding spectral slice using a standard digital coherent receiver [22]. At this point, DSP enables recombination of the spectral slices after electronic detection. In this transmission system, Δf_G can be different from Δf_M as long as the total measurement bandwidth

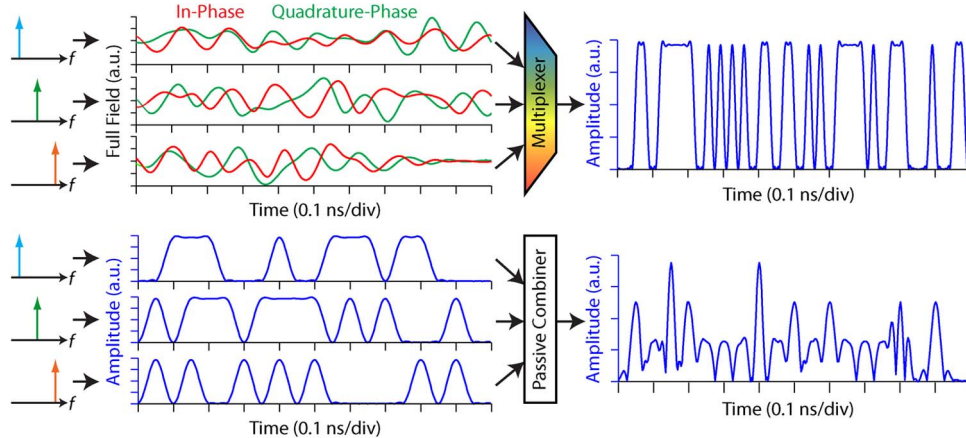


Fig. 2. Comparison between OAWG and CoWDM waveform generation. (a) OAWG combines seemingly random modulations together to form a target single-carrier (shown here) or multicarrier waveform. (b) CoWDM operates by combining many orthogonal subcarriers together to form a seemingly random waveform.

($M \times \Delta f_M$) is greater than the generated waveform's bandwidth ($N \times \Delta f_G$). The use of spectral slices enables independent optimization at the transmitter and receiver for the exact bandwidth of available electronics and allows utilization of the transmitters and receivers across heterogeneous network domains.

Generating waveforms by dividing the spectrum into spectral slices is an efficient means of generating large bandwidth waveforms using low bandwidth electronics, but the spectral domain processing requires *a priori* knowledge of the waveform for the entire time window. However, a continuous (i.e., infinite) duration waveform can be temporally divided into manageable time durations with the use of temporal slice filters. Analogous to spectral slice filters, temporal slice filters enable the temporary division of a continuous data waveform into temporal slices [17], [18], with a minimal effect on the generated waveform's fidelity. For example, a scenario in which each temporal slice has a duration equal to 30 periods of the OFC results in only 0.01% error while introducing a 2-ns DSP latency. The tradeoff between time slice duration (i.e., latency) and SNR penalty is detailed in [17], [18]. The Fourier transform of each time slice is then divided into spectral slices using the frequency slice filters, according to Fig. 1(a). The use of time slices enables minimization of size of the electrical buffers and FFT operations that would otherwise be required.

A dynamic OAWG transmitter and OAWM receiver based transmission system can generate and detect arbitrary waveforms in any modulation format within its operating bandwidth. As a result, in addition to being able to operate using a single carrier modulation format such as binary phase-shifted keying (BPSK) and quaternary phase-shifted keying (QPSK), it is also possible to utilize multicarrier modulation formats such as CoWDM and OFDM using the same transmitter and receiver structure. Furthermore, multicarrier waveforms can be generated with each carrier having a unique bandwidth and modulation format.

Additionally, the fact that dynamic OAWG and OAWM operate over a continuous, broadband spectrum enables compensation for both linear and nonlinear link impairments. For example, precompensation can be applied for certain impairment mechanisms (e.g., chromatic dispersion) at the transmitter (OAWG) to reduce the signal distortion at the receiver [23]. In addition, since the waveform spectra created using dynamic OAWG is completely predetermined, undesirably high peak-to-average power ratios (PAPR) can be avoided. Postcompensation is also possible at the receiver (OAWM) to reduce or eliminate undesirable linear and nonlinear link impairments since the receiver DSP operates over the full field of the broadband received signal. In particular, using an OAWM receiver and applying nonlinear back propagation to the entire spectrum yields improved impairment compensation over performing processing on a channel-by-channel basis [24].

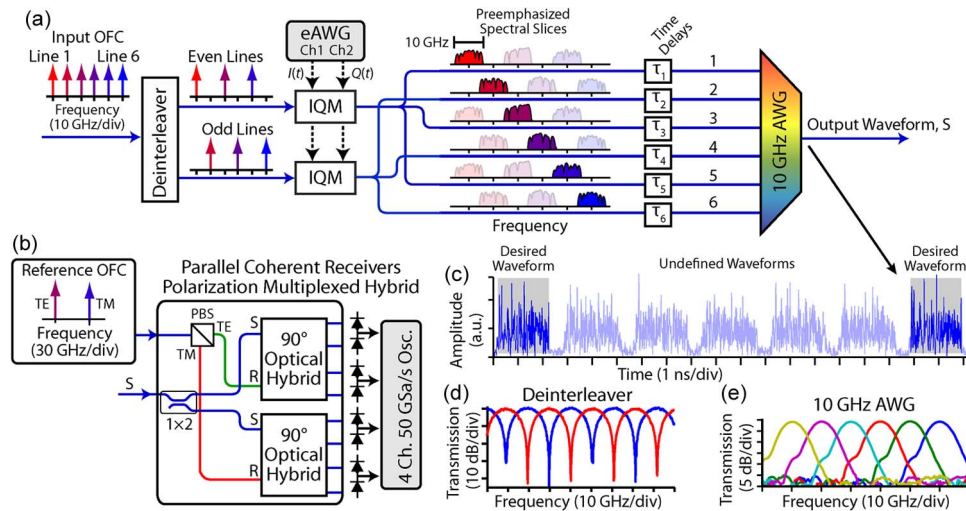


Fig. 3. Experimental arrangement for (a) 6×10 GHz spectral slice waveform generation and (b) 2×30 GHz spectral slice measurement. (c) Example output waveform generated with time interleaving scheme. Measured transmission for (d) deinterleaver and (e) AWG multiplexer. IQM: I/Q modulator. eAWG: Electronic arbitrary waveform generator. AWG: Arrayed-waveguide grating. OFC: Optical frequency comb.

Despite the similarity in structure to CoWDM [4] and OFDM [5] transmitters, there are fundamental differences with respect to a spectral slice transmitter. In particular, Fig. 2(a) shows the main operating principle of a spectral slice transmitter, which involves the coherent combination of many spectral slices. Here, the temporal real and imaginary modulations correspond to the inverse Fourier transform of each spectral slice [see Fig. 1(a), left]. Combining these seemingly random temporal spectral slice modulations together yields the desired output waveform, shown here in on-off keying (OOK) format, but can be in any modulation format including CoWDM or OFDM. Note that the bandwidth of individual spectral slices is independent of the bandwidth of subcarriers in the generated waveform.

Since the architecture of dynamic OAWG transmitter architecture closely resembles those of CoWDM and OFDM transmitters, it is important to point out their differences. As Fig. 2(b) shows, CoWDM orthogonally combines many low-speed subcarriers that have a constant phase relationship to each other to form a seemingly random output waveform. This example shows OOK CoWDM subcarriers, but the principle applies for coherent modulation formats as well. To maintain orthogonality between subcarriers, the CoWDM subcarrier symbol rate is set equal to the subcarrier frequency spacing, and therefore, each modulator can only generate an integer number of subcarriers. This is in contrast to dynamic OAWG, which only requires an integer number of subcarriers for the total transmitter bandwidth (i.e., not per modulator). Additionally, both CoWDM and dynamic OAWG transmitters can change the modulation format of individual subcarriers, but only dynamic OAWG allows manipulation of the whole transmitted bandwidth as a single entity. For ease of visualization in the time domain, Fig. 2(b) shows an example using CoWDM, but the same concepts also apply to no guard band OFDM.

3. Demonstration of an OAWG/OAWM Transmitter/Receiver System

3.1. Experimental Arrangement

Fig. 3 shows the experimental arrangement used to generate and measure single carrier and multicarrier data waveforms with 60 GHz of continuous bandwidth. Here, the dynamic OAWG transmitter generated 6×10 GHz spectral slices and the OAWM receiver detected 2×30 GHz

spectral slices. An OAWG transmitter using six spectral slices that is capable of continuous (infinite duration) data waveforms needs 12 independent analog signals to drive the six independent I/Q modulators. However, here we show a proof-of-principle six-slice demonstration of 2-ns long data waveforms using two I/Q modulators with 12-GHz of analog bandwidth and two independent outputs from an electronic arbitrary waveform generator (eAWG) that operates at 12 GS/s and has 5.5 GHz of analog bandwidth. Fig. 3(a) shows the details of the six-slice dynamic OAWG transmitter. First, a 10 GHz input OFC was generated using a combination of amplitude and phase modulation on a cw laser using a dual-electrode Mach–Zehnder modulator [25]. Six OFC lines were then isolated using a bandpass filter and sent to a spectral deinterleaver [Fig. 3(d)], which separated the “even” and “odd” comb lines to separate fibers. An eAWG generated the repetitive I and Q signals with a 16.67-ns period that were used to create the spectral slices. The modulated “even” and “odd” comb lines were each split three ways, and a time interleaving scheme enabled using the two independent eAWG outputs and two I/Q modulators to create the 12 independent signals (for 2 ns) necessary for the generation of the six spectral slices. Delaying the i th spectral slice by $\tau_i = i \times 2.8$ ns ensured that the six spectral slices were temporally synchronized for a 2-ns window within each 16.67-ns period [see Fig. 3(c)]. The remaining time within each period resulted in undefined waveforms and was ignored. The spectral slices were combined using a 10-GHz arrayed-waveguide grating (AWG) with broadened (i.e., strongly overlapping) passbands [see Fig. 3(e)] to produce the output waveform, S .

The 2-ns, 60-GHz output waveform, S , was amplified and detected in two 30-GHz slices using an OAWM receiver, which consisted of a reference OFC, polarization diversity optical hybrid, balanced detectors and real-time digitizing oscilloscope [see Fig. 3(b)] [19]. The reference OFC consisted of two comb lines (1 TE and 1 TM) separated by 30 GHz. The 2×30 -GHz spectral slices were retrieved using coherent detection followed by real-time digitization. Offline postprocessing enabled correction for optical hybrid imbalances, combination of the two slices, generation of eye and constellation diagrams, and bit-error-rate (BER) performance analysis.

For correct generation of desired waveforms, the phase between each spectral slice needed alignment. This proof-of-principle experimental setup based on fiber pigtailed components introduced slowly varying random phase shifts between the transmitter’s spectral slices. As a result, only measurements with the correct relative spectral slice phases were recorded (typically 1% of the data acquisitions for each waveform). Moving toward integrated photonic devices to implement spectral slice transmitters will ensure a constant phase relationship between spectral slices and allow for improved waveform fidelity [26], [27]. For waveform detection, phase alignment between receiver spectral slices was performed in the receiver DSP [19].

All transmitter and receiver DSP operations were performed offline using a PC. However, for real-time implementation, temporal slices are necessary to generate continuous time duration waveforms [17], [18]. Implementing continuous 60-GHz waveforms given the transmission system scenario described here, each 2-ns duration temporal slice would require one 120-element FFT operation and six 20-element IFFT operations at the OAWG transmitter. A continuous time OAWM receiver would require two 60-element FFT operations and one 120-element IFFT operation to reassemble the original waveform.

3.2. Single-Carrier Waveform

Using spectral slice based waveform generation and measurement it is possible to transmit and receive single carrier data waveforms with a total bandwidth much greater than that of the supporting electronics. Fig. 4 presents measured results for a 60-GHz, 2-ns single carrier BPSK data waveform. The use of a square modulation filter ensures increased spectral efficiency (1 b/s/Hz), but at the cost of increased time domain ripple. Fig. 4(a) shows the temporal waveform averaged over 119 frames, which indicates a close match between the measured data and target values. Fig. 4(b) shows the frequency domain of the 60-GHz data waveform, which shows close agreement with the target values. Fig. 4(c) and (d) present histogram based eye and constellation diagrams of the single carrier BPSK waveform. The open eye and separated constellation points show error free operation

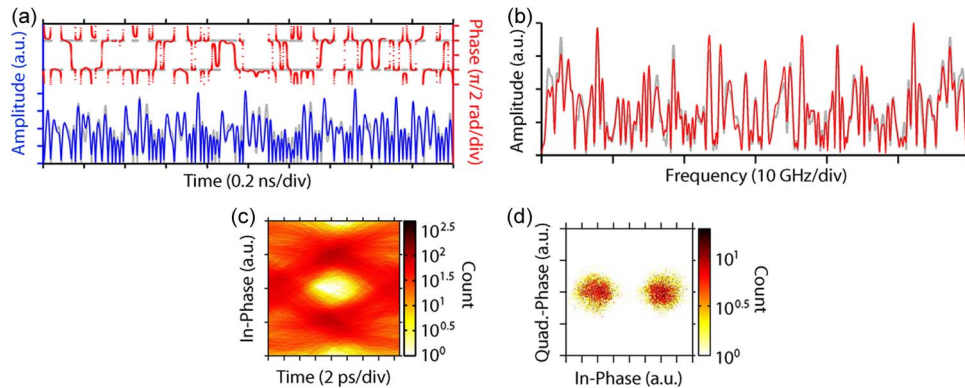


Fig. 4. Sixty-gigahertz, 120-bit, 2-ns BPSK waveform. (a) Time domain measured amplitude (blue) and phase (red) and target (gray) averaged over 119 frames and (b) corresponding spectrum. Histograms of the (c) eye diagram and (d) constellation diagram for 14 280 bits.

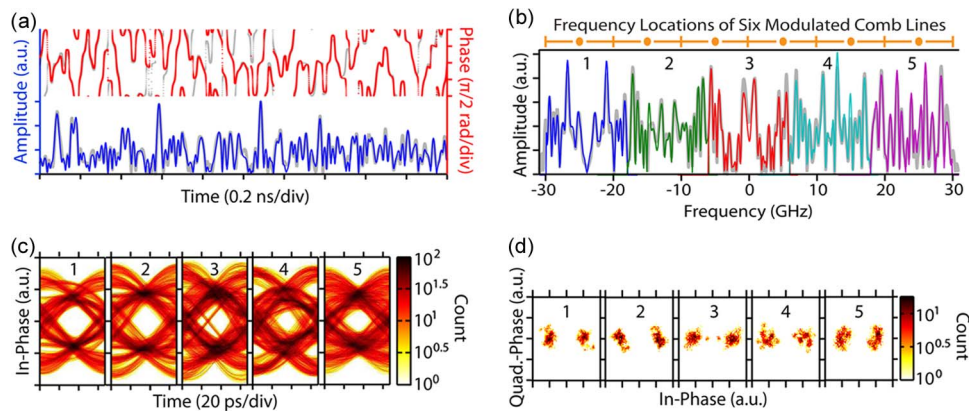


Fig. 5. Sixty-gigahertz, 2-ns, 120-bit, 1 b/s/Hz CoWDM waveform with five, 12-GHz BPSK subcarriers. (a) Time domain measured amplitude (blue) and phase (red) and target (gray) averaged over 119 frames and corresponding (b) spectrum. Colors indicate the five subcarrier spectra and target (gray). Histograms of the (c) eye diagrams and the (d) constellation diagrams for 2856 bits for each of the five subcarriers (14 280 bits total).

over the 14 280 bits tested indicating a BER below 7×10^{-5} . Variations in eye openness and constellation point separateness are dependent on waveform shaping accuracy, which led to small systematic errors. In this case, with a single channel transmission, the systematic errors are averaged over the entire waveform and cause reductions in the eye opening versus theory.

3.3. Multicarrier Coherent WDM Waveforms

This section presents experimental results for the generation and detection of multicarrier CoWDM waveforms with both five subcarriers and 15 subcarriers. A key significance of using spectral slice waveform generation and detection is that the spectral slices are not restricted to only generating an integer number of CoWDM subcarriers. In other words, using OAWG and OAWM it is possible to generate subcarriers with contributions from multiple adjacent spectral slices. This allows for precise matching between the bandwidth demand for a particular channel and allocated bandwidth. In the case of the five-subcarrier CoWDM waveform, each subcarrier was generated by two adjacent 10-GHz transmitter spectral slices, while each subcarrier in the 15-subcarrier CoWDM waveform was generated by a single 10-GHz transmitter spectral slice or by two adjacent spectral slices, depending on the subcarrier frequency location. Using the two 30-GHz receiver spectral

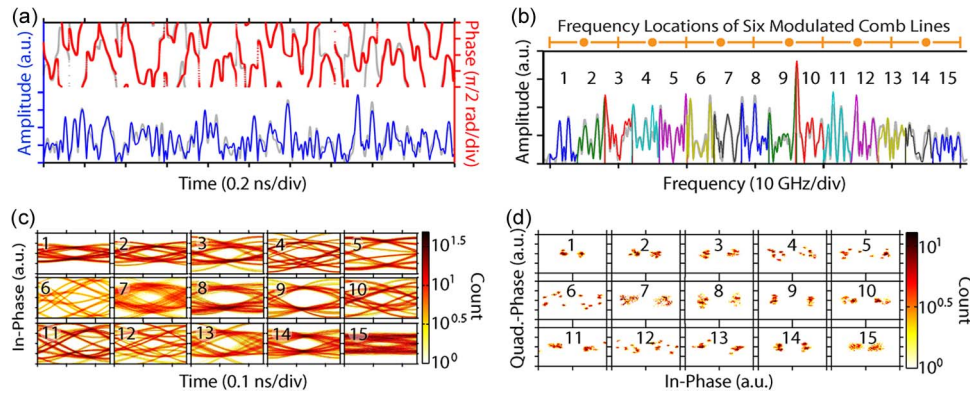


Fig. 6. Sixty-gigahertz, 120-bit, 2-ns CoWDM waveform with 15 BPSK subcarriers. (a) Time domain measured amplitude (blue) and phase (red) and target (gray) averaged over 119 frames and (b) corresponding spectrum. Colors indicate the five subcarrier spectra and target (gray). Histograms of the (c) eye diagrams and (d) constellation diagrams for 952 bits for each of the 15 subcarriers (14 280 bits total).

slices, each subcarrier for both the five- and 15-subcarrier CoWDM waveforms was detected using a single spectral slice, except the subcarrier in the middle, which was partially detected by both receiver spectral slices.

Fig. 5 shows measured results for the generation and measurement of a 60-GHz, 2-ns CoWDM waveform with five subcarriers, each consisting of 12-GHz BPSK signals. The use of a square modulation filter maximized the achievable BPSK spectral efficiency to 1 b/s/Hz. Orthogonality between subcarriers was guaranteed by setting the subcarrier symbol rate (12 GBd) to the subcarrier spacing (12 GHz). Fig. 5(a) shows the time domain of the five-subcarrier CoWDM waveform averaged over 119 acquisition frames versus the target. There is a close match between measured and target data that indicates high-fidelity waveform generation and measurement. In Fig. 5(b), the corresponding frequency domain occupying 60 GHz of bandwidth is superimposed on the target data. Colors and numbers indicate the bandwidth used to generate each of the subcarriers. Yellow dots denote the spectral locations of the six modulated comb lines at the transmitter. Slight mismatch between measured and target data can be mitigated through improved *I/Q* modulator calibration. Fig. 5(c) and (d) show the histogram based eye and constellation diagrams for each of the five subcarriers, which show open eyes and separated constellation points for 2856 bits per subcarrier for a total of 14 280 bits. Variations in the openness of the eyes and separation of the constellation points are a result of systematic errors that are directly related to the shaping accuracy of the subcarrier spectra. Error free operation for each subcarrier over the measured data indicates an overall BER $< 7 \times 10^{-5}$, well below the forward error correction (FEC) limit (BER = 10^{-3}) for the commonly used Reed–Solomon (255 239) code.

Fig. 6 shows measured results for a 60-GHz, 2-ns CoWDM waveform with 15 subcarriers. In this case, the 4-GHz subcarriers have a 4-GHz frequency spacing and consist of 4-GBd BPSK waveforms with a spectral efficiency of 1 b/s/Hz that was achieved using a square modulation filter. In Fig. 6(a), the measured waveform averaged over 119 frames is closely aligned in both amplitude and phase with the target values. In Fig. 6(b), the corresponding 60 GHz of spectrum contains each of the 15 spectral slices (colors and numbers). Some subcarriers were generated by one transmitter spectral slice alone (center positions indicated by yellow dots) and others by a combination of two adjacent spectral slices. Slight errors in *I/Q* modulator preemphasis and in phase alignment of the spectral slices resulted in varying degrees of difference between measured and target values for each subcarrier. Fig. 6(c) shows histogram based eye and constellation diagrams for 952 bits within each of the 15 subcarriers for a total of 14 280 bits. All eyes are open but with variations in the size of the eye opening directly related to systematic errors in the waveform shaping accuracy of the corresponding subcarrier. These systematic errors led to the result that certain subcarriers had

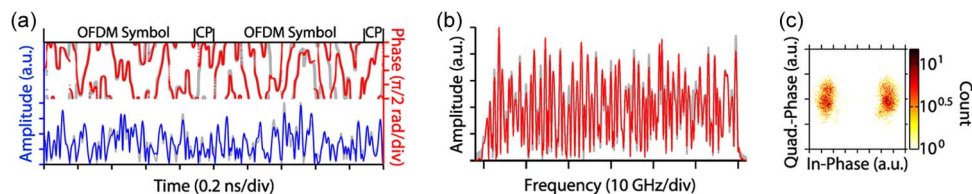


Fig. 7. Sixty-gigahertz, 108-bit, 2-ns, two-symbol OFDM waveform with 54 BPSK subcarriers and a cyclic prefix of 10% (0.1 ns). (a) Time domain measured amplitude (blue) and phase (red) and target (gray) averaged over 119 frames and (b) corresponding spectrum. Histogram of the (c) constellation diagram for 12 852 bits. CP: Cyclic prefix.

improved performance (i.e., larger eye openings). Fig. 6(d) presents constellation diagrams for each subcarrier, which show separated constellation points. Each subcarrier was error free over the measured data, which indicates an overall BER $< 7 \times 10^{-5}$.

3.4. Multicarrier OFDM Waveform

This section shows the capability of a spectral slice based transmission system to generate and measure a typical optical OFDM waveform with many subcarriers and a cyclic prefix (CP) [5]. Fig. 7 shows measured results for two, 1-ns symbols of a 60-GHz OFDM waveform with 54 BPSK subcarriers and a CP of 10% for an overall spectral efficiency of 0.9 b/s/Hz. Fig. 7(a) shows the time domain for the two symbol OFDM waveform averaged over 119 acquisition frames. The waveform is complex but shows a close agreement to target data with slight discrepancies due to inaccuracies in waveform shaping. In Fig. 7(b), the 60 GHz of continuous bandwidth of measured spectral amplitude overlaps well with the target values, which indicates successful waveform generation. Fig. 7(c) shows a histogram based constellation diagram for the superposition of all 54 subcarriers together for a total of 12 852 bits. The error-free operation of each subcarrier indicates an overall BER $< 7 \times 10^{-5}$ over the measured data.

4. Conclusion

In this paper, we presented an arbitrary modulation format and flexible bandwidth-capable transmission system based on a dynamic OAWG transmitter and an OAWM receiver that relies on the parallel synthesis and detection of multiple spectral slices. Experimental demonstrations utilized 6×10 GHz spectral slices to generate optical waveforms with 60 GHz of contiguous bandwidth, which were then detected in 2×30 GHz spectral slices. Experimental results yielded error-free transmission of single carrier waveforms, five-subcarrier CoWDM waveforms, 15-subcarrier CoWDM waveforms, and 54-subcarrier OFDM waveforms. These results provide experimental examples of how an OAWG transmitter and an OAWM receiver can satisfy the needs of flexible bandwidth networking by creating waveforms with arbitrary bandwidth that can be in either single carrier or multicarrier modulation formats. Also, in systems implemented with dynamic OAWG and OAWM, the transmitter and receiver spectral slice bandwidths are completely independent from each other and from the baud rate of the generated subcarriers. Furthermore, spectral slice based transmitters and receivers are a bandwidth-scalable technology, which enables an efficient matching between optical and electrical bandwidths. Further maturation of integrated device technology will enable Terahertz bandwidth flexible bandwidth-capable systems using dynamic OAWG transmitters and OAWM receivers on a single photonic chip [26], [27].

References

- [1] M. Jinno, B. Kozicki, H. Takara, A. Watanabe, Y. Sone, Y. Tanaka, and A. Hirano, "Distance-adaptive spectrum resource allocation in spectrum-sliced elastic optical path network," *IEEE Commun. Mag.*, vol. 48, no. 8, pp. 138–145, Aug. 2010.
- [2] K. Christodoulopoulos, I. Tomkos, and E. A. Varvarigos, "Elastic bandwidth allocation in flexible OFDM-based optical networks," *J. Lightw. Technol.*, vol. 29, no. 9, pp. 1354–1366, May 2011.

- [3] D. J. Geisler, R. Proietti, Y. Yin, R. P. Scott, X. Cai, N. K. Fontaine, L. Paraschis, O. Gerstel, and S. J. B. Yoo, "The first testbed demonstration of a flexible bandwidth network with a real-time adaptive control plane," *Proc. Eur. Conf. Optical Commun.*, 2011, Th. 13.K.2.
- [4] P. Frascella, N. M. Suibhne, F. C. G. Gunning, S. K. Ibrahim, P. Gunning, and A. D. Ellis, "Unrepeated field transmission of 2 Tbit/s multi-banded coherent WDM over 124 km of installed SMF," *Opt. Express*, vol. 18, no. 24, pp. 24 745–24 752, Nov. 2010.
- [5] W. Shieh and I. Djordjevic, *OFDM for Optical Communications*. Burlington, MA: Elsevier, 2010.
- [6] H. Takahashi, A. Al Amin, S. L. Jansen, I. Morita, and H. Tanaka, "Highly spectrally efficient DWDM transmission at 7.0 b/s/Hz using 8×65.1 -Gb/s coherent PDM-OFDM," *J. Lightw. Technol.*, vol. 28, no. 4, pp. 406–414, Feb. 2010.
- [7] D. Hillerkuss, T. Schellinger, R. Schmogrow, M. Winter, T. Vallaitis, R. Bonk, A. Marculescu, J. Li, M. Dreschmann, J. Meyer, S. Ben Ezra, N. Narkiss, B. Nebendahl, F. Parmigiani, P. Petropoulos, B. Resan, K. Weingarten, T. Ellermeier, J. Lutz, M. Moller, M. Huebner, J. Becker, C. Koos, W. Freude, and J. Leuthold, "Single source optical OFDM transmitter and optical FFT receiver demonstrated at line rates of 5.4 and 10.8 Tbit/s," presented at the Optical Fiber Commun. Conf., San Diego, CA, Mar. 21–25, 2010, Paper PDPC1.
- [8] B. Kozicki, H. Takara, Y. Tsukishima, T. Yoshimatsu, K. Yonenaga, and M. Jinno, "Experimental demonstration of spectrum-sliced elastic optical path network (SLICE)," *Opt. Express*, vol. 18, no. 21, pp. 22 105–22 118, Oct. 2010.
- [9] A. Sano, E. Yamada, H. Masuda, E. Yamazaki, T. Kobayashi, E. Yoshida, Y. Miyamoto, R. Kudo, K. Ishihara, and Y. Takatori, "No-guard-interval coherent optical OFDM for 100-Gb/s long-haul WDM transmission," *J. Lightw. Technol.*, vol. 27, no. 16, pp. 3705–3713, Aug. 2009.
- [10] Z. Jiang, C. Huang, D. E. Leaird, and A. M. Weiner, "Optical arbitrary waveform processing of more than 100 spectral comb lines," *Nat. Photon.*, vol. 1, no. 8, pp. 463–467, Aug. 2007.
- [11] K. Takiguchi, K. Okamoto, T. Kominato, H. Takahashi, and T. Shibata, "Flexible pulse waveform generation using silica-waveguide-based spectrum synthesis circuit," *Electron. Lett.*, vol. 40, no. 9, pp. 537–538, Apr. 2004.
- [12] Z. Jiang, D. E. Leaird, and A. M. Weiner, "Line-by-line pulse shaping control for optical arbitrary waveform generation," *Opt. Express*, vol. 13, no. 25, pp. 10 431–10 439, Dec. 2005.
- [13] P. J. Delyfett, S. Gee, M.-T. Choi, H. Izadpanah, W. Lee, S. Ozharar, F. Quinlan, and T. Yilmaz, "Optical frequency combs from semiconductor lasers and applications in ultrawideband signal processing and communications," *J. Lightw. Technol.*, vol. 24, no. 7, pp. 2701–2719, Jul. 2006.
- [14] N. K. Fontaine, R. P. Scott, J. Cao, A. Karalar, K. Okamoto, J. P. Heritage, B. H. Kolner, and S. J. B. Yoo, "32 phase \times 32 amplitude optical arbitrary waveform generation," *Opt. Lett.*, vol. 32, no. 7, pp. 865–867, Apr. 2007.
- [15] J. T. Willits, A. M. Weiner, and S. T. Cundiff, "Theory of rapid-update line-by-line pulse shaping," *Opt. Express*, vol. 16, no. 1, pp. 315–327, Jan. 2008.
- [16] M. Akbulut, S. Bhoopapur, I. Ozdur, J. Davila-Rodriguez, and P. J. Delyfett, "Dynamic line-by-line pulse shaping with GHz update rate," *Opt. Express*, vol. 18, no. 17, pp. 18 284–18 291, Aug. 2010.
- [17] N. K. Fontaine, "Optical arbitrary waveform generation and measurement," Ph.D. dissertation, Univ. California, Davis, Davis, CA, 2010.
- [18] R. P. Scott, N. K. Fontaine, J. P. Heritage, and S. J. B. Yoo, "Dynamic optical arbitrary waveform generation and measurement," *Opt. Express*, vol. 18, no. 18, pp. 18 655–18 670, Aug. 2010.
- [19] N. K. Fontaine, R. P. Scott, L. Zhou, F. M. Soares, J. P. Heritage, and S. J. B. Yoo, "Real-time full-field arbitrary optical waveform measurement," *Nat. Photon.*, vol. 4, no. 4, pp. 248–254, Apr. 2010.
- [20] D. J. Geisler, N. K. Fontaine, R. P. Scott, T. He, L. Paraschis, O. Gerstel, J. P. Heritage, and S. J. B. Yoo, "Bandwidth scalable, coherent transmitter based on the parallel synthesis of multiple spectral slices using optical arbitrary waveform generation," *Opt. Express*, vol. 19, no. 9, pp. 8242–8253, Apr. 2011.
- [21] D. J. Geisler, N. K. Fontaine, R. P. Scott, L. Paraschis, O. Gerstel, and S. J. B. Yoo, "Generation and detection of arbitrary modulation format, coherent optical waveforms scalable to a terahertz," presented at the IEEE Photonics Soc. Summer Topicals, Montreal, QC, Canada, Jul. 18–20, 2011, Paper MC4.3.
- [22] E. Ip, A. P. T. Lau, D. J. F. Barros, and J. M. Kahn, "Coherent detection in optical fiber systems," *Opt. Express*, vol. 16, no. 2, pp. 753–791, Jan. 2008.
- [23] D. J. Geisler, N. K. Fontaine, R. P. Scott, T. He, L. Paraschis, J. P. Heritage, and S. J. B. Yoo, "400-Gb/s modulation-format-independent single-channel transmission with chromatic dispersion precompensation based on OAWG," *IEEE Photon. Technol. Lett.*, vol. 22, no. 12, pp. 905–907, Jun. 2010.
- [24] E. Ip, "Nonlinear compensation using backpropagation for polarization-multiplexed transmission," *J. Lightw. Technol.*, vol. 28, no. 6, pp. 939–951, Mar. 2010.
- [25] T. Sakamoto, T. Kawanishi, and M. Izutsu, "Asymptotic formalism for ultraflat optical frequency comb generation using a Mach-Zehnder modulator," *Opt. Lett.*, vol. 32, no. 11, pp. 1515–1517, Jun. 2007.
- [26] F. M. Soares, J.-H. Baek, N. K. Fontaine, X. Zhou, Y. Wang, R. P. Scott, J. P. Heritage, C. Junesand, S. Lourduoss, K. Y. Liou, R. A. Hamm, W. Wang, B. Patel, S. Vatanapradit, L. A. Gruezeke, W. T. Tsang, and S. J. B. Yoo, "Monolithically integrated InP wafer-scale 100-channel \times 10-GHz AWG and Michelson interferometers for 1-THz-bandwidth optical arbitrary waveform generation," presented at the Optical Fiber Commun. Conf., San Diego, CA, Mar. 21–25, 2010, Paper OThS1.
- [27] N. K. Fontaine, R. P. Scott, and S. J. B. Yoo, "Dynamic optical arbitrary waveform generation and detection in InP photonic integrated circuits for Tb/s optical communications," *Opt. Commun.*, vol. 284, no. 15, pp. 3693–3705, Jul. 2011.